



Photolytic Degradation of Herbicide Atrazine by Radiation Ultraviolet (UVC): An Application of Green Chemistry

Valmir Felix de Lima^{1*}, Francisco Sávio Gomes Pereira^{2*},
Alexandre Ricardo Pereira Schuler¹, Maria de Los Angeles P. F. Palha¹,
Antonio Demóstenes de Sobral¹, Iranildo José da Cruz Filho¹
and Agrinaldo Jacinto do Nascimento Junior³

¹Department of Chemical Engineering, Federal University of Pernambuco – UFPE, Center of Technology and Geosciences, Recife, PE, Brazil.

²Federal Institute of Education, Science and Technology of Pernambuco – IFPE, Campi Recife and Ipojuca, PE, Brazil.

³Federal Institute of Education, Science and Technology of Paraná – IFPR, Campus Paranavaí, Paranavaí, PR, Brazil.

Authors' contributions

This work was carried out in collaboration between all authors. Authors VFL, AJNJ and IJCF participated in the execution of laboratory experiments. Authors MLAPFP, ARPS and ADS participated in literature review and planning of the article. Authors VFL and FSGP participated in writing and text editing. All authors read, reviewed and approved the text of article.

Article Information

DOI: 10.9734/CSJI/2016/29619

Editor(s):

(1) Jaya Narayan Sahu, Petroleum and Chemical Engineering Programme Area, Institut Teknologi Brunei (ITB), National Engineering and Technology University, Brunei Darussalam.

(2) Pradip K. Bhowmik, Department of Chemistry, University of Nevada Las Vegas Maryland Parkway, Las Vegas NV, USA.

Reviewers:

(1) Anonymous, Lebanese University, Lebanon.

(2) Endang Tri Wahyuni, Gadhah Mada University, Indonesia.

(3) Ayansina Ayantade Dayo Victor, Bowen University, Nigeria.

Complete Peer review History: <http://www.sciencedomain.org/review-history/16968>

Original Research Article

Received 21st September 2016
Accepted 15th November 2016
Published 19th November 2016

ABSTRACT

Atrazine (ATZ) is an herbicide of the s-triazines classes used on crops as corn, cotton, soybean, and sugar cane. This work shows the ATZ degradation by ultraviolet radiation (UVC, 254 nm) in a bench-scale annular photoreactor. The initial concentration of the irradiated samples ranged from 2.0×10^{-5} to 1.2×10^{-4} mol·L⁻¹. Actinometry was used to determine the radiant energy incident on the

*Corresponding author: E-mail: valmir.lima@ufpe.br, cientista.francisco@yahoo.com.br;

photoreactor (1.36×10^{-9} einstein \cdot cm $^{-2}$ \cdot s $^{-1}$) and the radiation source was a low-pressure mercury vapor discharge lamp with tubular glass (Phillips TUV 36 W). The conversion in 240s (27.5% - 48.7%) is related inversely with the concentration of the samples. Some results found: photochemistry reaction rate (0.9×10^{-9} to 2.2×10^{-9} mol \cdot cm $^{-3}$ \cdot s $^{-1}$), volumetric rate of photon absorption (VRPA) (2.0×10^{-8} to 8.0×10^{-8} einstein \cdot cm $^{-3}$ \cdot s $^{-1}$), and global initial quantum yield (0.03 to 0.05 mol \cdot einstein $^{-1}$). For the reaction rate was proposed a phenomenological model and the process was modeled of form deterministically. The estimated values for the kinetic parameters ϕ_{atz} , m, and n were, respectively: 0.03 mol \cdot einstein $^{-1}$, 0.02 and 0.5. The kinetic model fitted the data with accuracy of 91.8%. As conclusion of the work, the photolytic degradation with UVC is an efficient process, low cost and can be used to set up pilot plants, in various scales, to reduce or eliminate compounds of the atrazine class or similar emerging contaminants, in effluents.

Keywords: Atrazine; agricultural pesticides; emerging contaminants; environmental pollution; green chemistry; irradiation treatment.

1. INTRODUCTION

The environmental contamination of aquatic systems by agricultural pesticides is a problem that has aroused the interest of the scientific community. The issue is that herbicides molecules are difficult to degrade, show great mobility in the environment, and has been detected both in surface water and ground water. Brazil is today one of the largest herbicides consumers of the world. This fact is mainly due to agricultural model used and biological variety cultivated, which favors the incidence of pests [1,2].

The Brazilian Institute of Geography and Statistics (IBGE) [3] found that the crops of corn, sugarcane, cotton, and soybeans uses approximately 75% of all herbicide marketed in Brazil, with 39% of this total has in its composition Atrazine (2-chloro-4-ethylamino-6-isopropylamino-1,3,5-triazine) (Fig. 1) as active agent. Atrazine is classified as a herbicide from the group of s-triazines, molar mass 215.7 g \cdot mol $^{-1}$, water solubility of 33 mg \cdot L $^{-1}$ at 25°C, melting point of 171-174°C and density of 1.187 g \cdot cm $^{-3}$ at 20°C [4].

The Brazilian Ministry of Health (Ordinance n.2914/2011) establishes the concentration of 2 μ g \cdot L $^{-1}$ de Atrazine (ATZ) as the maximum value acceptable in water for the human consumption [5]. ATZ has high persistence in soil, and slow hydrolysis, resulting as your major metabolite, the hydroxyatrazine (HA). For mammals, the contact with ATZ may cause cancer and mutagenic effects and still may act as one endocrine disruptor [6]. This agricultural pesticide, as a chemical compound, can be classified as emerging contaminant along with

pharmaceuticals, cleaning products, industrial chemicals and others. It can contaminate the handler direct or indirect way through the air (agricultural pesticide applicators), water and food (fruit and vegetables) [7].



Fig. 1. Atrazine (2-chloro-4-ethylamino-6-isopropylamino-1,3,5-triazine)

The Brazilian National Water Resources Council - CNRH (Motion n. 61 of 10/07/2012) recommends to all public, private organizations, and especially the agencies of development and funding to research, in promoting actions to improve the quality control, on treatments of drinking water, and effluents, these efforts aim in removing emerging pollutants, improvement in identification techniques, monitoring and quantification of organic compounds [8].

The Green Chemistry concept emerged in the 1990s and was aimed at reducing pollution by using so-called green solvents. Planning chemical processes to obtain a final product that would use the same amount of input materials (atom economy and catalysis) is essential to the Green Chemistry approach. In 1998, Anastas and Warner proposed a set of twelve Green Chemistry principles that would serve as guidelines, and these guidelines would be focused on reducing the waste that was generated during chemical processes, using non-toxic solvents, applying catalysts (when possible), and designing chemical processes in

accordance with the principle of atom economy [9]. The Principles of Green Chemistry can be illustrated as: 1. Prevention of waste; 2. Atom economy; 3. Less hazardous synthesis; 4. Safer chemicals; 5. Safer solvents and auxiliaries; 6. Energy efficiency - Energy requirements should be recognized for their environmental and economic impacts and should be minimized. Synthetic methods should be conducted at ambient temperature and pressure; 7. Renewable feedstocks; 8. Reduce derivatives; 9. Catalysis - Catalytic reagents (as selective as possible) are superior to stoichiometric reagents; 10. Design for degradation - Chemical products

should be designed so that at the end of their function they do not persist in the environment and break down into innocuous degradation products; 11. Real-time analysis for pollution prevention; 12. Inherently safer chemistry for accident prevention [10].

One possible treatment for elimination or reduction of these emerging contaminants (in the case, the atrazine) in non treated water or effluent is the photo-oxidation [11], contemplated, with adaptations in the principles 6, 9 and 10 of the Green Chemistry. The photo-oxidation (Fig. 2) reactions happen due to electronic excitations

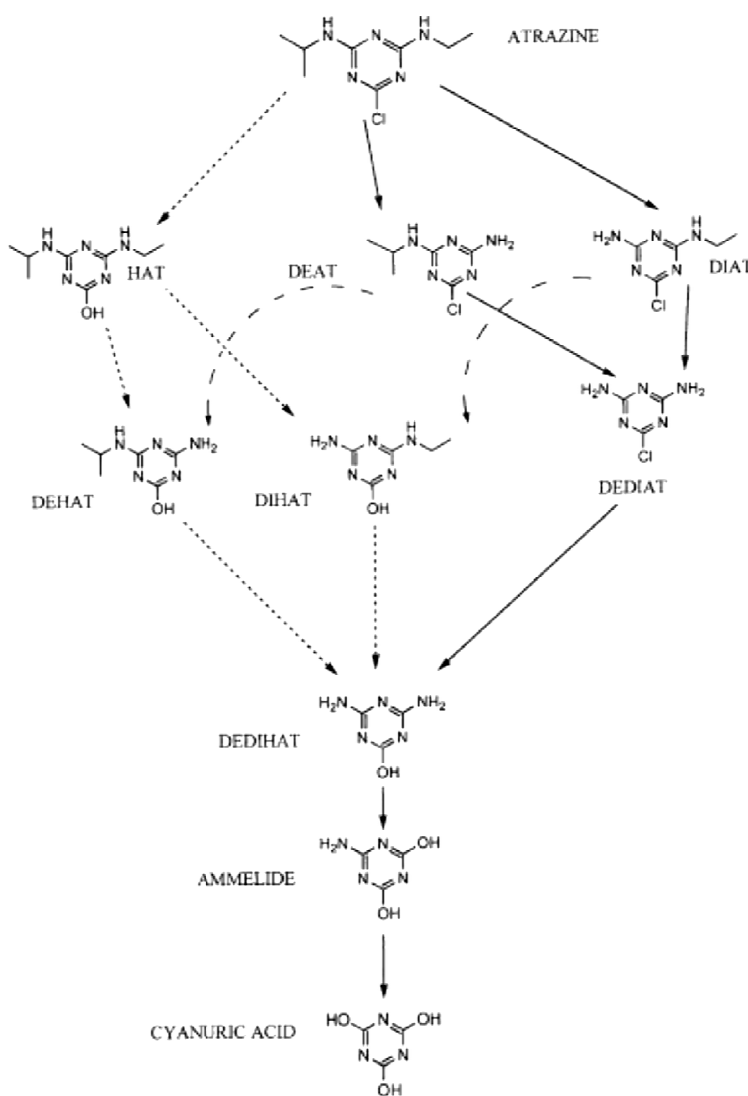


Fig. 2. Pathways of atrazine degradation under ozonation and photocatalysis (full arrows), direct photolysis at 254 nm (dotted arrows) and photolytic ozonation at 254 nm (full, dotted and dashed arrows) [14]

of organic substances via radiant energy absorption. Many times, implies in a electron transfer from the excited state to ground-state molecular oxygen, followed by recombination of the radical ions, or hydrolysis of the radical cation, or homolysis forming radicals which then react with oxygen [12]. The yield is low for a photo-oxidation of an organic compound in aqueous phase using low pressure mercury lamp (254 nm), however, some methods have considerable efficiency. Since 1980s the decontamination of polluted water by organic compounds via direct photolysis at 254 nm is studied [13].

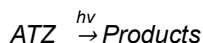
The aim of this study was to develop kinetic study of the degradation of Atrazine, via direct photolysis at 254 nm, with accompanying formation of metabolites, and verification of deterministic model developed based on the incidence model for the process.

2. MATERIALS AND METHODS

2.1 Modeling

2.1.1 Kinetic model

The kinetic scheme for the direct photolysis at 254 nm Atrazine is given by:



As a photochemical process, the photobleaching rate of a compound i , as ATZ, may be displayed by a simple phenomenological model [15,16] which proposes that this rate be a function on the average concentration of i ($\langle C \rangle$).

$$\langle R_i(t) \rangle = -\phi_i [\langle C_i(t) \rangle]^m [\langle e_\lambda^a(t) \rangle]^n \quad (1)$$

Where: ϕ_i : quantum yield of i ; m , and n : kinetic parameters.

2.1.2 Concentration profile

The balance of matter for one species (i) of a system in recycle [17] is given by:

$$V_R \frac{\partial}{\partial t} \langle C_i(t) \rangle_{V_R} + V_T \frac{\partial}{\partial t} \langle C_i(t) \rangle_{V_T} = V_I \langle R_i(t) \rangle_{V_R} \quad (2)$$

Where: " i " is the specie to be degraded (ATZ); $\langle C_i(t) \rangle_{V_R}$, and $\langle R_i(t) \rangle_{V_R}$, are respectively, concentration rate and average degradation rate of i .

Miranda [18] developed the model for the dynamic differential profile for the specie i considering the experimental system used in this work, according with Equation 3:

$$\frac{dC_i(t)}{dt} = \frac{V_I}{V_T} \langle R_i(t) \rangle_{V_R} \quad (3)$$

Initial condition:

$$t = 0 \rightarrow C_i(0) = C_i^0 \quad (4)$$

2.1.3 Radiation field properties

Models developed for incident radiation [19], and VRPA for the species i , according incidence model [16], are as follows:

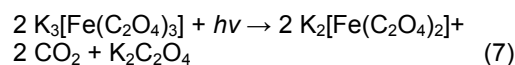
$$\langle G_\lambda(t) \rangle_{V_R} = \frac{2 r_q}{\kappa_T(t)[r_p^2 - r_q^2]} G_w \{1 - \exp[-\kappa_T(t)(r_p - r_q)]\} \quad (5)$$

$$\langle e_\lambda^a(t) \rangle_{V_R} = \frac{2 \kappa_i(t) r_q}{\kappa_T(t)[r_p^2 - r_q^2]} G_w \{1 - \exp[-\kappa_T(t)(r_p - r_q)]\} \quad (6)$$

Where: G_w radiant energy incident on the optical input of reactor, r_p e r_q radii of the Pyrex and quartz tubes, respectively; $\kappa_T(t)$ coefficient of total absorption to 254nm, $\kappa_T(t) = \sum_i^n \alpha_i C_i$; κ_i coefficient of absorption incident volumetric, at 254 nm from specie i , $\kappa_i(t) = \alpha_i C_i$; α_i , and α_n neperian molar absorptivity at 254 nm of i , and all absorbing species (i -n), and all species present in the reagent mixture, respectively.

2.1.4 Incident radiation on the optical input of reactor

The incident radiation on the input of reactor (G_w) can be accurately measured by actinometry (measuring of radiation intensity in the reaction evolution), and used as standard chemical the potassium ferrioxalate [20,21] associated with balance of matter on actinometer [22]. The reaction, in its simplified form, is given by:



The actinometric reaction kinetics [12] can be described by:

$$\langle R_{Fe^{2+},\lambda}(r,t) \rangle_{V_R} = \phi_{Fe^{2+},\lambda} \langle e_\lambda^a(t) \rangle_{V_R} \quad (8)$$

Where: $\phi_{Fe^{2+}}$ at 254 nm is $1.25 \text{ mol}\cdot\text{einstein}^{-1}$ [20].

The ions Fe^{3+} and Fe^{2+} absorb radiation at 254nm, $\alpha_{\text{Fe}^{3+}} = 4992 \text{ mol}^{-1}\cdot\text{cm}^{-1}$, and $\alpha_{\text{Fe}^{2+}} = 2560 \text{ mol}^{-1}\cdot\text{cm}^{-1}$ [20]. Therefore, the Equation 6, takes the following form [16]:

$$\langle e_{\lambda}^a(t) \rangle_{V_R} = \frac{2 \kappa_{\text{Fe}^{3+}}(t) r_q}{[\kappa_{\text{Fe}^{3+}}(t) + \kappa_{\text{Fe}^{2+}}(t)] [r_p^2 - r_q^2]} G_w \left\{ 1 - \exp[-[\kappa_{\text{Fe}^{3+}}(t) + \kappa_{\text{Fe}^{2+}}(t)](r_p - r_q)] \right\} \quad (9)$$

Early in the process, converting Fe^{2+} is in the range from 1 to 12%, resulting $\kappa_{\text{Fe}^{2+}}$ be approximately equal to zero, the radiation is absorbed mainly by the Fe^{3+} ($\kappa_{\text{Fe}^{3+}} \gg 1$). Based on these facts, Silva [19], simplified the Equation 9, obtaining the model for the incident radiation on the optical input of photoreactor.

$$G_w = \frac{1}{\phi_{\text{Fe}^{2+}} A_I} \left(\frac{dC_{\text{Fe}^{2+}}}{dt} \right)_{t \rightarrow 0} \quad (10)$$

Where: A_I , and V_I are respectively, irradiated area, and irradiated volume.

2.2 Experimental - Reagents and Equipment

ATZ was provided by Novartis-Syngenta (98% purity). The patterns of the ATZ metabolites (MT), deethylatrazine (DIA), desisopropylatrazine (DEA), and desethyldeisopropylatrazine (DAA) were all from Merck. The other reagents used were of analytical grade (Merck) and for preparation of solutions patterns deionized water was used.

The degradation process of ATZ (via direct photolysis at 254 nm) was performed in a annular photoreactor specially designed for the development of kinetic studies (Fig. 3). The reactor is part of a closed loop system consists of a recycle tank (effective volume 8.000 cm^3) stirred mechanically (Agitator from Fisaton, model 715), a magnetic centrifugal pump (Bomax, MaxMag model MD-10 L), and a heat exchanger connected to a thermostatic bath. The sampling port was installed on the outlet pipe of

the recycle tank, 3 cm from its base. As emission source was used a mercury germicidal lamp of low pressure from Phillips, model TUV-36W. Table 1 lists information on the degradation system (photoreactor, recycle tank, and germicidal lamp).

Aqueous solutions of ATZ (8,000 cm^3) were prepared from a stock solution with a concentration of $1.3 \times 10^{-4} \text{ mol}\cdot\text{L}^{-1}$. The concentrations of the initial solutions of the experiments varied of $2.0 \times 10^{-5} \text{ mol}\cdot\text{L}^{-1}$ to $1.2 \times 10^{-4} \text{ mol}\cdot\text{L}^{-1}$ (pH = 7) and were submitted to direct photolysis process at 254 nm. The lamp was turned on and maintained during 1800s (30 min.) before the photodegradation process for its stabilization (emission and temperature). The flow of recycle solution was maintained set at $58.8 \text{ cm}^3\cdot\text{s}^{-1}$. The system temperature was maintained at $26 \pm 1^\circ\text{C}$, by means of cooling system with heat exchanger and thermostatic bath. Samples were collected in two time intervals, 120 s ($T_p \leq 600$ s), and 600s ($T_p \geq 600$ s), in order to obtain the dynamic evolutions of the following process parameters: (a) volumetric absorption coefficient of ATZ, and its MT; (b) concentration of ATZ and its MT.

The value G_w was determined by potassium ferrioxalate actinometry in according to [23]. System operating conditions in photobleaching: volume, 8,000 cm^3 ; flow rate, $58.8 \text{ cm}^3\cdot\text{s}^{-1}$; agitation, 1,000 rpm; temperature, $26 \pm 1^\circ\text{C}$; pH 7; actinometer concentration (potassium ferrioxalate), $6 \text{ mmol}\cdot\text{L}^{-1}$. Samples from evolving reaction were collected during the processing period 720s at regular interval of 120s, starting in $t = 0$ s. The values of neperian molar absorptivity coefficient (α) of Fe^{3+} , and Fe^{2+} are respectively, $4,992 \text{ mol}^{-1}\cdot\text{cm}^{-1}$, and $2,560 \text{ mol}^{-1}\cdot\text{cm}^{-1}$. The Fe^{2+} concentration was obtained by colorimetry at 510 nm (UV-VIS spectrophotometer, from SP, Model 2000-UV) after having been complexed by 1.10-phenanthroline, according to the analytical method proposed by [20].

Table 1. Information on system Atrazine degradation

Item	Parameter	Value
Photoreactor	External radii of quartz tube	2.2 cm
	Internal diameter of the Pyrex [®] tube	3.0 cm
	Cross section from irradiated	1.3 cm^2
	Length	48 cm
	Irradiated volume (V_I)	610 cm^3
Recycle tank	Effective volume (V_T)	$8,000 \text{ cm}^3$
Lamp (Phillips TUV-36 W)	Rated power	36 W
	Power at 254 nm	9.0 W

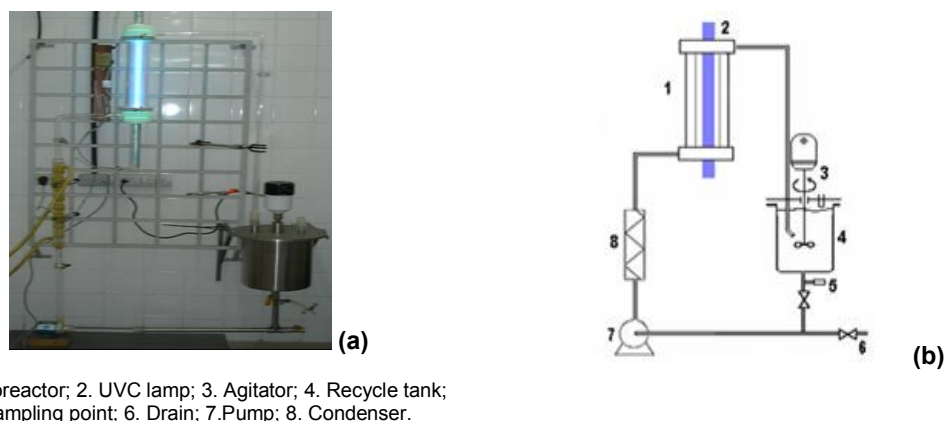


Fig. 3. Annular photoreactor used for to degrade the atrazine
(a) Reactor in operation (b) Simplified scheme

A Shimadzu A10 series HPLC (Shimadzu, Kyoto, Japan), and a pump CG 480 was used to determine the ATZ concentration, and their MT. The samples were loaded on a C18 Nucleosil® column (250 by 4.6 mm, 5 μm -diameter particles, 120 Å). Isocratic elution was performed at a flow rate of 1 mLmin^{-1} , mobile phase of methanol /water (70:30, v/v), and injection volume of 20 μL . The neperian molar absorptivity of ATZ and its MT at 254 nm were obtained using UV-VIS spectrophotometer from SP, Model 2000-UV.

3. RESULTS AND DISCUSSION

Table 2 shows the absorptivities, molar (ϵ_i), and molar neperian (α_i) at 254 nm obtained for the ATZ and its most important MT.

It can be seen from Table 2 that both the ATZ as their MT absorb UV radiation, at 254 nm, being ATZ and DEA the compounds that more absorb such radiation. These results indicate that the attenuation of UVC radiation will be caused not only by Atrazine, but also by their MT, as they are formed during the photodegradation process.

Table 2. Optical parameters of ATZ, and its MT at 254 nm

Species	ϵ_i ($\text{mol}^{-1}\cdot\text{cm}^{-1}$)	α_i ($\text{mol}^{-1}\cdot\text{cm}^{-1}$)
ATZ	4296.9	9894.0
DEA	4070.2	9372.0
DIA	3496.4	8051.0
DAA	2854.8	6573.0

Fig. 4 shows the dynamics evolution for the Fe^{2+} and Fe^{3+} concentrations on the first 840 s of UV

irradiation, at 254 nm. The potassium ferrioxalate actinometry technique was applied accurately, because $X_{\text{Fe}^{+2}}$ ranged from 1 to 12% [20].

According to approach introduced on section 2.4, the value of the term $\lim_{t \rightarrow 0} \left[\frac{dC_{\text{Fe}^{2+}}(t)}{dt} \right]$ given in

Equation 11 is defined as the slope of Fe^{2+} concentration versus time (Fig. 3b), equals $1.9 \times 10^{-9} \text{ mol}\cdot\text{s}^{-1}$. Consequently, the value of radiant energy incident on the optical input of photoreactor, G_w , is equal to $1.36 \times 10^{-9} \text{ einstein}\cdot\text{cm}^{-2}\cdot\text{s}^{-1}$.

$$E^w = \frac{V_T}{\phi_{\text{Fe}^{2+}}} \left[\frac{dC_{\text{Fe}^{2+}}}{dt} \right]_{t \rightarrow 0} = \frac{A_I}{V_I} V_T G_w \quad (11)$$

The value obtained in this work for G_w was similar to that obtained by [16] who worked with similar experimental system using the same type of lamp and flow conditions, to study the inactivation of *Escherichia coli* by UVC radiation. This agreement is perfectly justifiable; since the overall time of lamp usage was 800 h. Silva [16] presented a discussion about the accuracy of this measure on the basis of data provided by the manufacturer for the radiant power at 254 nm (E^w), which can be calculated using data from the potassium ferrioxalate actinometry, and the Equation 11 [16]. Table 3 shows the comparative results for the lamp used in the study.

The discrepancy between, the power values provided by the manufacturer, the values found by [19], and the calculated in this work (Equation 11) is due to radiation attenuation experienced in pass through the wall of the quartz tube whose refractive index is 1.52. The G_w value found is considered of excellent accuracy.

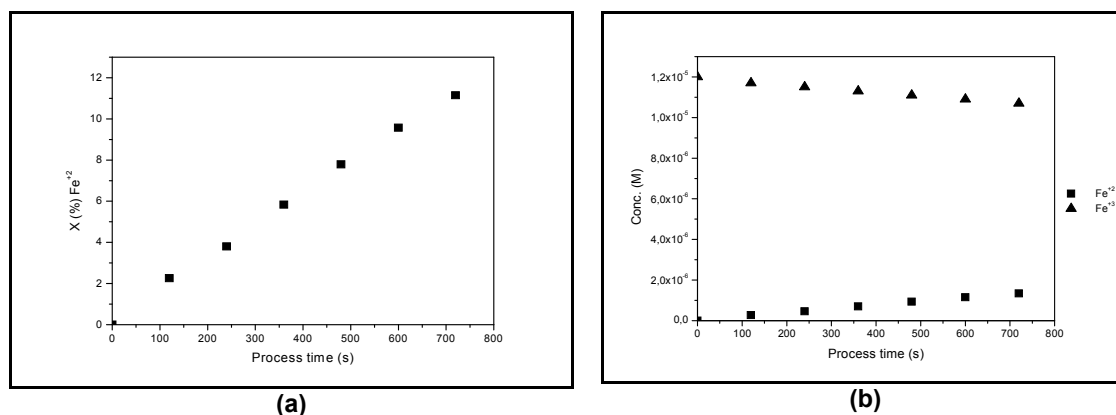


Fig. 4. (a) Conversion of $X(\text{Fe}^{+2})$ to $X(\text{Fe}^{3+})$; (b) dynamics evolution for the Fe^{2+} and Fe^{3+} concentrations

Table 3. Comparison on the power from study lamp

Manufacturer data*			Data obtained in accordance with equation 11			
Nominal power (W)	L nominal (cm)	Power at 254 nm (W)	L net (cm)	Net power at 254 nm ** (W)	Input power of photoreactor*** (W)	Percentage of loss
36	119.9	14.6	48.0	5.84	5.61	3.94

*Source: www.philips.com; **Value obtained based on vendor data; ***Value obtained by Eq. 11; L – Length of the lamp

Table 4. Process efficiency parameters

$C_{Atr}^o \times 10^5$ ($\text{mol}\cdot\text{L}^{-1}$)	$X_{240\text{ s}}$ (%)	$\langle R_{\lambda}^{t \rightarrow 0} \rangle \times 10^9$ ($\text{mol}\cdot\text{cm}^{-3}\cdot\text{s}^{-1}$)	$\langle e_{\lambda}^q(t) \rangle_{t \rightarrow 0} \times 10^8$ ($\text{einstein}\cdot\text{cm}^{-3}\cdot\text{s}^{-1}$)	$\phi_{t \rightarrow 0}^*$ ($\text{mol}\cdot\text{einstein}^{-1}$)
2,0	48,7	0,9	2,0	0,05
5,5	38,5	1,5	4,0	0,04
11,4	27,5	2,2	8,0	0,03

*Defined as $\phi_{t \rightarrow 0} = \frac{\langle R_{\lambda}^{t \rightarrow 0} \rangle}{\langle e_{\lambda}^q(t) \rangle_{t \rightarrow 0}}$ [27]

Fig. 5 shows the dynamic evolution for the ATZ concentrations, to the initial concentrations of $2.0 \times 10^{-5} \text{mol}\cdot\text{L}^{-1}$, $5.5 \times 10^{-5} \text{mol}\cdot\text{L}^{-1}$, and $11.4 \times 10^{-5} \text{mol}\cdot\text{L}^{-1}$, and its DEA (MT) to the condition in which the initial concentration of atrazine was $5.5 \times 10^{-5} \text{mol}\cdot\text{L}^{-1}$, along the atrazine's direct photolysis process at 254 nm.

As can be seen in Fig. 5a, the decay curves of the concentration of Atrazine with the photodegradation process time are classic exponential. Suggest that the degradation rate of ATZ decreases as the initial concentration increases this herbicide, which is in agreement with the literature. From Fig. 5b it is seen that the ATZ used suffered some type of photolysis previously, once detected the presence of DEA in the model solution at a concentration of $1.9 \times 10^{-5} \text{mol}\cdot\text{L}^{-1}$, which represents 34.5% the initial Atrazine's concentration ($5.5 \times 10^{-5} \text{mol}\cdot\text{L}^{-1}$). It is also noted that during the initial 240 s of the

process, DEA, and ATZ were photolysed, however, there is no production of this MT. The remaining MT, DIA and DAA, were not detected. After this processing period, the AED metabolite is produced and degraded simultaneously. These results are consistent with those obtained by [24].

Table 4 above shows the influence of atrazine's initial concentration on efficiency parameters of the process obtained when the time tending to zero, that is, average reaction rate, VRPA, $\langle e_{\lambda}^q(t) \rangle_{t \rightarrow 0}$, overall quantum yield, $\phi_{t \rightarrow 0}$ at 240 s of process (conversion). These parameters were evaluated at initial conditions of the process since the photoreactors are designed in these conditions, and to minimize inevitable errors, due to the anisotropy of the radiation field on such parameters when obtained at different times [25,26].

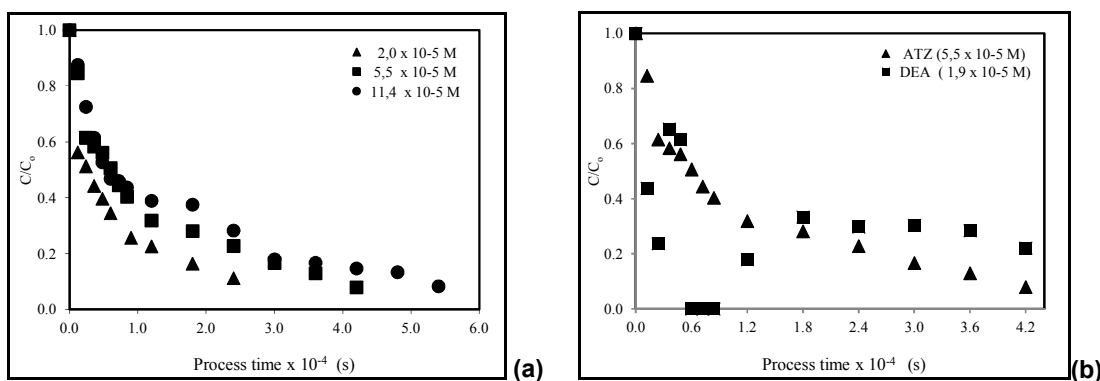


Fig. 5. (a) Dynamic evolution for ATZ concentrations; (b) Dynamic evolution for DEA concentrations

($T = 26 \pm 1^\circ\text{C}$, initial pH: 7,0; $G_w = 1.36 \times 10^{-9}$ einstein $\text{cm}^{-2} \cdot \text{s}^{-1}$)

The key property in a photochemical process is the VRPA [16], which in turn, have a temporal dependence with the concentration by the neperian volumetric coefficients of absorption, κ_i e κ_T (Equation 6). This fact can embed any dependency that the efficiency parameters of process can apparently not present in the initial concentration from specie i. The data presented in Table 4 indicate that the conversion of the ATZ in the process beginning (240s) is inversely proportional to the initial concentration of this herbicide, and the VRPA taken at the beginning of the process ($t \rightarrow 0$). On the other hand, the initial reaction rate was shown to be a direct function of these process parameters, confirming the proposition of Equation 1.

The overall quantum yield is a typical property of photochemical systems, and relates the utilization of photons absorbed towards achieving the desired goal. In this case, the ATZ's degradation, as well as on the nature of the reaction mechanism, that is, if it is high indicates that reaction occurs in chain, if small indicates that occurred, for example, deactivation or recombination [16]. Therefore, it can be stated that: a) during the photolysis reaction may have occurred deactivation processes, recombination or others who diverted the absorbed photons of their goal, since the value of $\phi_{t \rightarrow 0} < 1$ in all conditions investigated (Tabela 4); b) for the same irradiation condition, the overall quantum yield is higher for the operating condition in which the VRPA is smaller, that is, one where the initial concentration of atrazine is $2.0 \times 10^{-5} \text{ mol} \cdot \text{L}^{-1}$. This effect is produced by dependence of the order (n) on the VRPA (Equation 1) [25].

The parameters of the Equation 1, ϕ_{atz} , m, and n was estimated using the Runge-Kutta method

associated with the box optimization method, being respectively their values equal to 0.03 $\text{mol} \cdot \text{einstein}^{-1}$, 0.02, and 0.5. These results confirm that the degradation rate of ATZ via direct photolysis at 254 nm, is a direct function of their concentration and VRPA, being the influence of this last parameter on the reaction rate enhanced by reaction order, n. Fig. 6 shows the comparison between the simulated and experimental values for the concentration of ATZ. The developed model estimated the values for concentration of ATZ with 8.2% error.

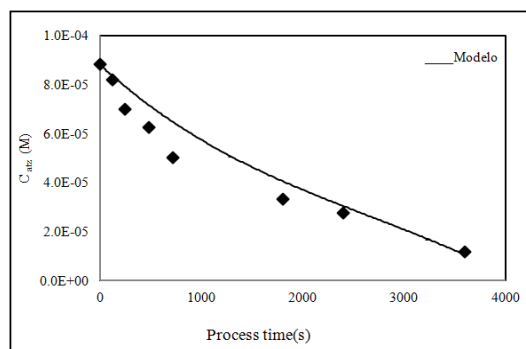


Fig. 6. Dynamic evolution for atrazine herbicide versus model

($T = 26 \pm 1^\circ\text{C}$; $G_w = 1.36 \times 10^{-9}$ einstein $\text{cm}^{-2} \cdot \text{s}^{-1}$; pH: 7.0)

4. CONCLUSIONS

This study indicated that direct photolysis reaction for the ATZ degradation not occurred in chain, so the process can undergo deactivation, or a molecular recombination. The kinetics of the process was evaluated according to an adapted model originally developed by [19], applying the incidence model to the process. The proposed kinetic model does not involve products, has

brought good results that serve as the primary basis for the reactor project. The results indicated mainly, the effect of VRPA on atrazine degradation rate by direct photolysis at 254 nm is enhanced by the dependence of that parameter with order n. As implementation perspective of this study on photolytic degradation is to set up pilot plants, in all scales, to reduce or eliminate compounds of atrazine class or similar emerging contaminants in effluents.

ACKNOWLEDGEMENTS

The authors thank the technical staff and managers of the Laboratory LCI of Department of Chemical Engineering of the UFPE by the support during the experiments this work and Novartis-Syngenta by donation of pesticide standards.

COMPETING INTERESTS

Authors have declared that no competing interests exist.

REFERENCES

1. Galli A, Souza D, Garbellini GS, Coutinho CFB, Mazo LH, Avaca LA, Machado SAS. Utilização de técnicas eletro-analíticas na determinação de pesticidas em alimentos. *Quim. Nova.* 2006;29(1):105-112. Portuguese
2. Pignati W, Oliveira NP, Silva AMC. Vigilância aos agrotóxicos: Quantificação do uso e previsão de impactos na saúde-trabalho-ambiente para os municípios brasileiros. *Ciência Saúde Coletiva.* 2014;19(12):4669-4678. Portuguese
3. IBGE IBGE. Produção Agrícola. (Accessed 20 June 2016)
Available:www.ibge.gov.br/home/estatistic/a/indicadores/agropecuaria/lspa/default.shtm Portuguese
4. Beltrán FJ, Ovejero G, Acedo B. Oxidation of atrazine in water by ultraviolet radiation combined with hydrogen peroxide. *Water Resource.* 1993;27(6):1013-1021.
5. BRASIL. Portaria nº 2914-12.12.2011. Ministério da Saúde. Procedimentos de controle e de vigilância da qualidade da água para consumo humano e seu padrão de potabilidade. (Accessed 20 June 2016)
Available:http://site.sabesp.com.br/uploads/file/asabesp_doctos/kit_arsesp_portaria2914.pdf Portuguese
6. Delduque MC, Marques SB, Silva LR. A reavaliação do registro de agrotóxicos e o direito à saúde. *Revista de Direito Sanitário.* 2010;11(1):169-175. Portuguese
7. Dams RI. Pesticidas: Usos e perigos à Saúde e ao meio ambiente. *Health and Environmental Journal.* 2006;7(2):57-65. Portuguese
8. BRASIL. Diário Oficial da União, nº 156 – DOU – 14/08/12 – seção 1 – p.36. Portuguese
9. Wiczerzak M, Namieśnik J, Kudłak B. Bioassays as one of the Green Chemistry tools for assessing environmental quality: A review. *Environment International.* 2016; 94:341–361.
10. Warner JC, Cannon AS, Dye KM. Green chemistry. *Environmental Impact Assessment Review.* 2004;24:775–799.
11. Dal Bosco SM, Barbosa IM, Candello FP, Maniero MG, Rath S, Guimarães JR. Degradation of ivermectin by Fenton and photo-Fenton and toxicity test using *Daphnia similis*. *Journal of Advanced Oxidation Technologies.* 2011;14(2):292-301.
12. Legrini O, Oliveros E, Braun AM. Photochemical processes for water treatment. *Chem. Rev.* 1993;93(2):671-698.
13. Lima VF. Cinética do processo de degradação do herbicida atrazina pelo processo avançado de oxidação H₂O₂-UVC. (Dissertação de Mestrado). Universidade Federal de Pernambuco; 2010. Portuguese
14. Bianchi CL, Pirola C, Ragaini V, Elena Selli E. Mechanism and efficiency of atrazine degradation under combined oxidation processes. *Applied Catalysis B: Environmental.* 2006;64:131–138.
15. Cabrera MI, Martín CA, Alfano OM, Cassano AE. Photochemical decomposition of 2,4 – dichlorophenoxyacetic acid (2,4-D) in aqueous solution. I. Kinetic Study, *Wat. Sci. Tech.* 1997;35(4):31-39.
16. Cassano AE, Martín CA, Brandi RJY, Alfano OM. Photoreactor analysis and design: Fundamentals and Applications. *Ind. Eng. Chem. Res.* 1995;34(7):2155-2220.

17. Bird RB, Stewart WE, Lightfoot EN. Fenômenos de transporte. 2. ed. Rio de Janeiro: LTC; 2004. Portuguese
18. Miranda JTG. Degradação do herbicida atrazina via processos oxidativo avançados. (Dissertação de Mestrado). Universidade Federal de Pernambuco; 2003. Portuguese
19. Silva AB. Desinfecção de água contaminada com *Escherichia coli*: Desenvolvimento de reator e estudo cinético. (Dissertação de Mestrado). Universidade Federal de Pernambuco; 2007. Portuguese
20. Murov SL, Carmichael I, Hug G. Handbook of photochemistry, 2. ed. New York: Marcel Dekker; 1993.
21. Pozdnyakov IP, Kel OV, Plyusnin VF, Grivin VP, Bazhin NM. New insight into photochemistry of ferrioxalate. J. Phys. Chem. A. 2008;112(36):8316–8322.
22. Zalazar CS, Labas MD, Martín CA, Brandi RJ, Alfano OM, Cassano AE. The Extended use of actinometry in the interpretation of photochemical reaction engineering data. Chemical Engineering Journal. 2005;109:67-81.
23. Romero RL, Alfano OM, Cassano AE. Cylindrical photocatalytic reactors radiation absorption and scattering effects produced by suspended fine particles in an annular space. Ind. Eng. Chem. Res. 1997;36: 3094–3109.
24. Hèquet V, Gonzalez, C, Le Cloirec P. Photochemical processes for atrazina degradation: Methodological approach. Wat. Res. 2001;35(18):4253-4260.
25. Labas MD, Brandi RJ, Martín CA, Cassao AE. Kinetics of bacteria inactivation employing UV radiation under clear water conditions. Chemical Engineering Journal. 2006;121:135-145.
26. Brandi RJ, Citroni MA, Alfano OM, Cassano AE. Absolute quantum yields in photocatalytic slurry reactors. Chemical Engineering Science. 2003;58(3-6):979-985.
27. Calvet JG, Pitts Jr JN. Photochemistry. London: Wiley & Sons; 1966.

© 2016 Lima et al.; This is an Open Access article distributed under the terms of the Creative Commons Attribution License (<http://creativecommons.org/licenses/by/4.0>), which permits unrestricted use, distribution, and reproduction in any medium, provided the original work is properly cited.

Peer-review history:
The peer review history for this paper can be accessed here:
<http://sciencedomain.org/review-history/16968>